

# Microstructure of the Copolymer Chain Generated by Anionic Ring-Opening Polymerization of a Model Cyclotrisiloxane with Mixed Siloxane Units<sup>1</sup>

M. Cypriak, K. Kaźmierski, W. Fortuniak, and J. Chojnowski\*

Center of Molecular and Macromolecular Studies, Polish Academy of Sciences, Sienkiewicza 112, 90-363 Łódź, Poland

Received July 29, 1999; Revised Manuscript Received December 13, 1999

**ABSTRACT:** Sequencing of siloxane units was studied in the copolymer chain formed by anionic polymerization of 2,2,4,4-tetramethyl-6,6-diphenylcyclotrisiloxane. The study involved three polymerization systems: lithium silanolate in THF, potassium silanolate complexed with 18-crown-6 in toluene, and tetramethylammonium silanolate in toluene. The sequencing proved to be a very good diagnostic tool for the studies of polymerization chemoselectivity. In all the three mentioned systems the chemoselectivity was high. In particular, processes leading to chain cleavage, such as backbiting and chain fragment interchange, occurred at a much lower rate than propagation, which allowed for quantitative studies of regioselectivity in polymerization. The pentad analysis, performed using the first-order Markov statistics, completed by the determination of the unit sequence at chain extremities, permitted the determination of the contributions from the monomer ring openings at three nonequivalent sites. The regioselectivity is poor as the ring is opened in each of these three places with a significant probability. The results provide important information on the mechanism of the chain propagation. They point to the role of the counterion assistance to the monomer ring opening. The generation of a more stable silanolate propagation center may also be important for choosing the site of the ring-opening. Ab initio calculations suggest the direct interaction of the phenyl group with the metal cation.

## Introduction

Controlled synthesis of siloxane–siloxane copolymers has attracted considerable attention, as the mixing of two or more types of siloxane units in a polymer chain is often necessary to obtain a material with the required properties.<sup>2–4</sup> However, the generation of these copolymers of well-defined structure may be a difficult task.

There are three general routes to siloxane–siloxane copolymers based on the ring-opening polymerization. The equilibrium copolymerization, often referred to as coequilibration, is the most commonly used route.<sup>1–7</sup> This process produces copolymers with a random<sup>6</sup> or nearly random<sup>1</sup> distribution of siloxane units, obeying Bernoulli statistics. The copolymerization leads to a considerable amount of cyclic oligomers, particularly, if substituents at silicon are bulky or polar,<sup>8,9</sup> or if the process is carried out in solution. Although the molecular weight may be controlled using a chain stopper, the polydispersity is large,  $\bar{M}_w/\bar{M}_n \geq 2$ . The process does not give any possibility for selective functionalization of one chain end, either.

The kinetically controlled, quenched copolymerization of two comonomers has been exploited.<sup>1–4,10–13</sup> This process is difficult to control, as a usually large difference in the reactivity of comonomers leads to a kinetic preference of one monomer over the other in addition to the growing polymer chain.<sup>3,11,13</sup> A block or gradient copolymer structure is usually obtained.

The siloxane–siloxane copolymers are also generated in the homopolymerization of cyclic siloxanes having at least two types of siloxane units. This method is particularly attractive when cyclotrisiloxanes are used as monomers. The anionic polymerization of these

cyclics, quenched at a suitable moment, may lead to a high yield of copolymers with a narrow molecular weight redistribution.<sup>9,14–21</sup> The copolymers have a uniform composition of siloxane units which also are uniformly spread along the copolymer chain. In addition, the copolymers selectively functionalized at one chain end may be obtained by using a functional initiator or a functional terminator.

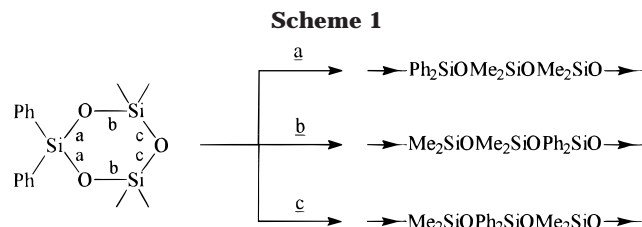
Although the polymerization of cyclotrisiloxanes with mixed units has been exploited in the synthesis of various siloxane copolymers,<sup>1,14–21</sup> there is little data on the microstructures of copolymer chains formed by this reaction. It was suggested in some earlier reports<sup>16,17</sup> that the polymerization led to copolymers of regular alternating structures, which implied that the monomer was always opened at the same site during propagation of the polymer chain. Our experience shows that this must have been a rather rare case.<sup>1,9,15,20</sup>

The purpose of this work is to study the polymerization of a model cyclotrisiloxane with two different units, initiated by some typical initiators of anionic polymerization, to check to what extent the copolymer sequencing may be controlled in this polymerization system. Studies of the sequencing of siloxane units give information about chemoselectivity and regioselectivity of the polymerization, thus providing valuable knowledge on the mechanism of this reaction.

## Results and Discussion

**Model.** The model monomer was 2,2,4,4-tetramethyl-6,6-diphenylcyclotrisiloxane, **1**. The monomer is a crystalline compound relatively easy to synthesize and purify.<sup>1,9</sup> Phenyl substituents are electron-withdrawing by an inductive effect, showing the value of the Taft parameter  $\Sigma\sigma^* = 1.2$ , compared to  $\Sigma\sigma^* = 0$  for methyl substituents. Thus, the presence of two phenyl groups

\* To whom correspondence should be addressed. E-mail: jchojnow@bilbo.cbmm.lodz.pl.



was expected to significantly differentiate the electrophilicities of the silicon centers in **1**. Using a monomer symmetrically substituted at silicon avoided complications related to stereochemistry. Sequences of the diphenylsiloxane and dimethylsiloxane units, denoted by X and D, respectively, were studied by  $^{29}\text{Si}$  NMR spectroscopy using a technique ensuring quantitative integration. The copolymer of diphenylsiloxane and dimethylsiloxane has already been the subject of earlier  $^{29}\text{Si}$  NMR studies.<sup>3,22</sup> Peaks of pentads were found to be well-resolved and the assignment of these peaks was performed giving access to study of the sequencing of siloxane units in this copolymer.

Three initiating systems of the anionic polymerization were used in this study, that is, a lithium silanolate in THF, a potassium silanolate with 18-crown-6, and a tetramethylammonium silanolate. All of them are known to promote the selective polymerization of hexamethylcyclotrisiloxane.<sup>23</sup> Thus, we hoped that the polymerization of monomer **1** could be chemoselectively performed, avoiding side processes of chain cleavage, such as backbiting and chain fragment interchange which are known to occur in equilibration of polysiloxanes. Chemoselectivity was required to make a deeper quantitative analysis of the sequencing of siloxane units, providing information about the regioselectivity of polymerization.

**Chemoselectivity of Polymerization.** Studies on the sequencing of siloxane units in the polymer, based on precision  $^{29}\text{Si}$  NMR investigation, may provide a diagnostic tool for the chemoselectivity of polymerization. In the chemoselective process, the sequencing is exclusively controlled by the way in which the monomer ring is opened and added to the growing polymer. There are three nonequivalent sites of the ring opening, marked in Scheme 1 by a, b, and c, which leads to three arrangements of siloxane units in the open monomer segment added to the polymer chain (Scheme 1).

In any case, the cyclic trimer enters the open polymer chain undivided. Thus, even if the addition occurred completely at random, with an equal probability for all three modes of the ring opening and independently of the structure of the chain end, the sequencing of the siloxane units in the copolymer would be much more specific than that in the copolymer obtained by the equilibrium polymerization of monomer **1**. The schematic representations of the  $^{29}\text{Si}$  NMR spectra of the copolymers, generated on those two routes, are compared in Figure 1. These spectra were calculated for the  $\text{Ph}_2\text{SiO}$  resonance region on the basis of the assignment of peaks determined earlier.<sup>22</sup> The spectrum of the copolymer formed by equilibration contains 10 signals representing the 16  $\text{Ph}_2\text{SiO}$ -centered pentads. Six out of these 10 signals do not appear on the spectrum of the copolymer obtained by quenched chemoselective polymerization of **1** with the random monomer addition. Thus, the absence of these signals is the criterion of the chemoselectivity of the process.

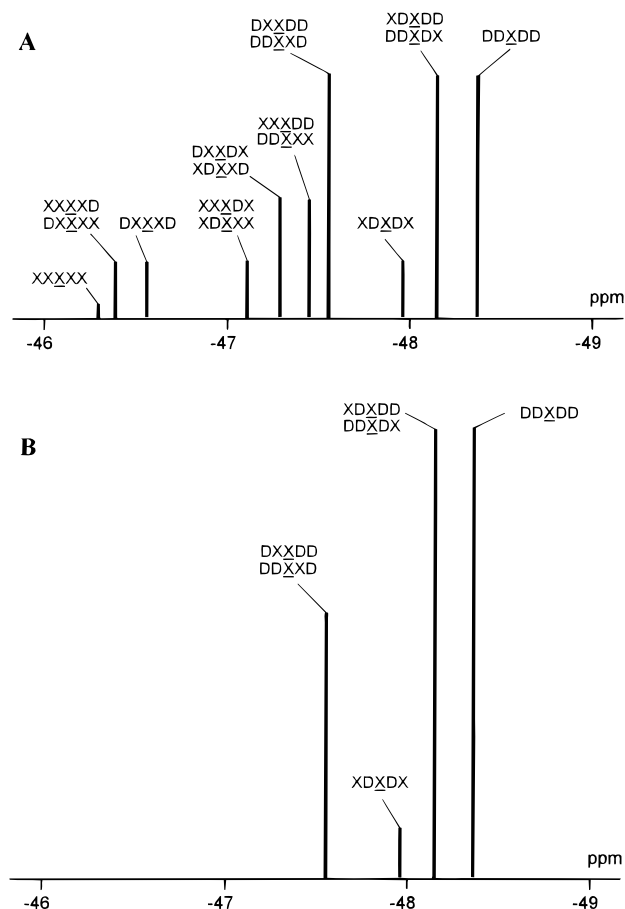


**Figure 1.** Schematic representation of  $^{29}\text{Si}$  NMR spectra of dimethylsiloxane-*co*-diphenylsiloxane in the range of the  $\text{Ph}_2\text{SiO}$  resonance region. D and X denote the  $\text{Me}_2\text{SiO}$  and  $\text{Ph}_2\text{SiO}$  units, respectively: (A) copolymer obtained by the equilibrium polymerization of monomer **1**, assuming that full randomization of the distribution of siloxane units occurred; (B) copolymer obtained by quenched anionic chemoselective polymerization of **1**, assuming that random ring opening occurred in the polymerization.

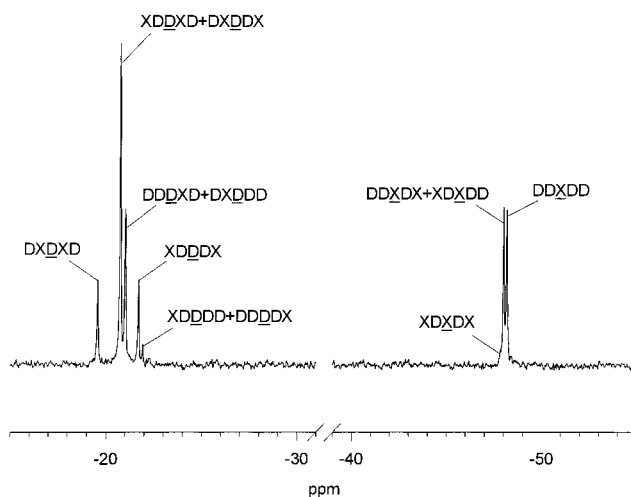


**Figure 2.**  $^{29}\text{Si}\{^1\text{H}\}$  NMR spectrum of poly[ $\text{Me}_2\text{SiO}$ -*co*- $\text{Ph}_2\text{SiO}$ ] obtained by chemoselective-quenched polymerization of monomer **1** initiated by  $\text{BuMe}_2\text{SiOLi}$  in THF.

The  $^{29}\text{Si}$  NMR spectrum of the copolymer obtained by quenched polymerization of **1** in THF, initiated with  $\text{BuMe}_2\text{SiOLi}$ , is shown in Figure 2. The signals of the forbidden pentads are absent, although the spectrum was taken at a high monomer conversion. The signal

**Table 1. Chemoselectivity of the Anionic Polymerization of Monomer 1 and Pentad Composition in the Copolymer<sup>a</sup>**

polymerization system propagation center/solvent/temp.	percent of allowed pentad for chemoselective process	contribution from allowed pentads (in % of total allowed pentads) values computed by Monte Carlo method are given in parantheses <sup>b</sup>											
		X	X	D	X	D	X	D	D	X	X	D	
		D	D	X	X	X	X	X	D	D	D	D	
		D	D	D	D	D	D	D	X	X	X	X	
		D	D	D	D	D	D	X	D	D	D	X	
		D	X	D	D	X	X	D	D	D	X	D	
~Me <sub>2</sub> SiOLi/THF/50 °C	100	2.0	7.5	16.7	0	32.2	0	8.3	17.1	15.0	1.2	0	
		(1.9)	(7.2)	(16.0)	(0.4)	(32.4)	(0.2)	(8.6)	(16.5)	(15.5)	(0.8)	(0.5)	
~Me <sub>2</sub> SiOK + 18-crown-6, 1:1/toluene/50 °C	99	6.1	3.7	11.7	3.3	36.1	2.7	3.5	18.0	7.8	1.5	5.5	
		(6.1)	(3.9)	(10.8)	(3.1)	(35.8)	(2.5)	(4.4)	(19.5)	(7.6)	(0.6)	(5.6)	
~Me <sub>2</sub> SiONMe <sub>4</sub> /toluene/30 °C	99	8.1	5.2	14.4	4.8	24.9	4.2	5.15	14.5	9.85	2.4	6.5	
		(8.6)	(5.1)	(14.7)	(4.1)	(24.6)	(3.4)	(6.2)	(14.8)	(9.7)	(1.3)	(7.5)	

<sup>a</sup> Polymerization was quenched at 60–90% of monomer conversion. Molecular weight of copolymer  $\bar{M}_n$  was about  $2 \times 10^4$  g mol<sup>-1</sup>. <sup>b</sup> For details see Experimental Section.

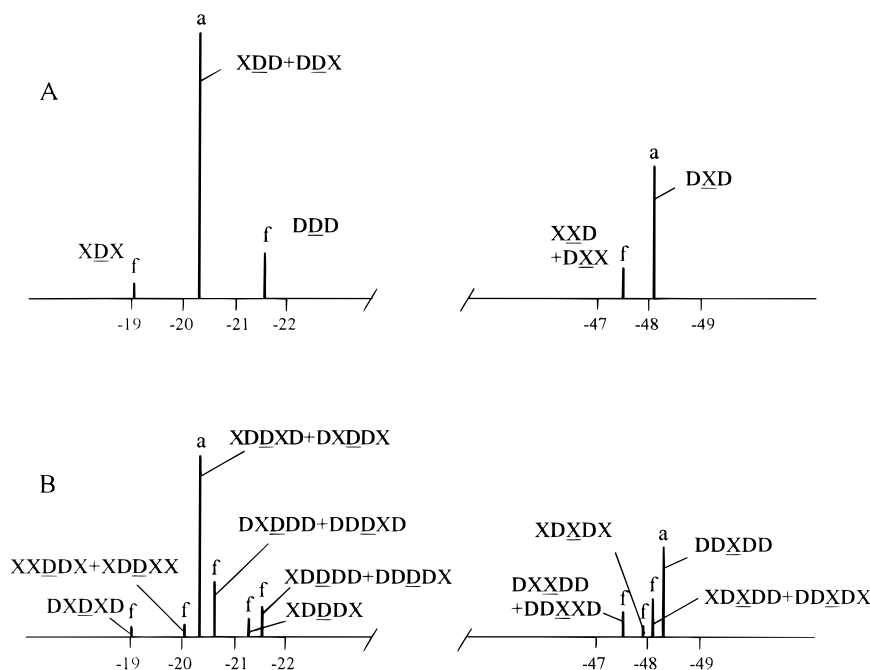


**Figure 3.** Schematic representation of <sup>29</sup>Si NMR spectra of poly[Me<sub>2</sub>SiO-*co*-Ph<sub>2</sub>SiO] obtained by the quenched polymerization of monomer 1 initiated by a potassium silanolate – 18-crown-6 complex in THF. Sequences allowed and forbidden for the regioselective polymerization are marked by “a” and “f”, respectively: (A) resolution at triad level; (B) resolution at pentad level.

pattern does not change with conversion up to at least 90%. The process is highly selective. The absence of signals for the forbidden pentads provides evidence that links between diorganosiloxane units in the copolymer chain are preserved during polymerization. Thus, backbiting and chain scrambling occur at a much lower rate than propagation. The sequencing of siloxane units in the polymer chain is not affected by the cleavage of the terminal diorganosiloxane unit either.

The chemoselectivity is high for all three systems of the anionic polymerization of 1 studied here. The comparison is made in Table 1 in terms of the percentage of the allowed pentads. Polymerization on potassium silanolate without any promoter occurs with a somewhat lower selectivity, 94%, which is in agreement with the previous results,<sup>9</sup> where significant amounts of cyclic oligomers were observed in a similar polymerization system. This lower selectivity corroborates the concept of multicentered interaction of the potassium cation with polysiloxane, promoting backbiting and chain randomization.<sup>23,24</sup> In a chemoselective polymerization system this interaction is reduced either by a competitive interaction of the counterion with a stronger nucleophile, that is, promoter or solvent, or by the

structure of the counterion which makes the multicenter interaction with polysiloxane impossible. Tetramethylammonium cation is an example of such an ion.

**Regioselectivity of Polymerization.** Because the electrophilic character of silicon centers in monomer 1 is differentiated by the inductive effect of phenyl substituents, one could expect a high regioselectivity of polymerization. If the monomer was opened exclusively in one of the three nonequivalent places, then the process would occur fully regioselectively, producing a copolymer with a perfectly regular arrangement of units with phenyl substituents at every third silicon atom. The impression that the structure of the copolymer is close to regular may, sometimes, arise from the shape of a low-resolution <sup>29</sup>Si NMR spectrum of the copolymer, where only triads are resolved (see Figure 3A). The signals of the triads characteristic for a regular structure may overwhelm those forbidden for this structure. However, in a high-resolution spectrum, the signals of the triads are split into signals of pentads, some of which are forbidden. An example is schematically shown in Figure 3B. It may be deduced from the inspection of the high-resolution spectra of the copolymers that, for

**Table 2. Dependencies of Triad Contents on Probabilities of Ring Opening at a, b, and c Based on the Bernoulli Statistics**

percent contribution from triads	dominating addition		
	a	b	c
[DDD]	100/3 ( $2P_b + P_c$ )	100/3 ( $2P_a + P_c$ )	100/3 ( $2P_a + P_b$ )
[XDD] + [DDX]	200/3 $P_a$	200/3 $P_b$	200/3 $P_c$
[XDX]	100/3 $P_c$	100/3 $P_c$	100/3 ( $P_a + P_b$ )
[XXX]	0	0	0
[DXX] + [XXD]	200/3 $P_b$	200/3 $P_a$	0
[DXD]	100/3 ( $P_a - P_b + P_c$ )	100/3 ( $P_b - P_a + P_c$ )	100/3 ( $P_a + P_b + P_c$ )

all the polymerization systems studied here, the regioselectivity is rather poor and the monomer ring is opened at various sites.

Determination of the relative rates of monomer **1** ring opening at a, b, and c in the chain propagation requires precise data on the sequence composition and tedious calculations based on statistical methods, completed by some additional experiments.

**Statistical Methods of Determination of the Siloxane Unit Sequencing.** In the most simple approach, an addition of a monomer, independent of the active propagation center, was assumed. Further simplification was accepted that the chain was almost regular; that is, one way of the ring opening was strongly preferred and its probability  $P_{\text{main}} \approx 1$ , where the main opening might have been at a site a, b, or c. The remaining two additions occur with probabilities  $P_{\text{pert}}$  low enough to be regarded as isolated perturbations along a chain, that is,  $P_{\text{pert}} \ll P_{\text{main}}$ , and the conditional probability  $P_{\text{main/pert}} = 1$ . The above assumptions lead to simple equations for the triad distribution in a chain, as shown in Table 2. From these equations, it is clear that the presence of the XXD triad implies the main opening at a or b, while the lack of this triad implies the main opening at c. However, the equation sets are symmetrical with respect to  $P_a$  and  $P_b$ ; hence, two or more equivalent solutions exist for each triad distribution. Thus, the simplified Bernoulli model cannot provide any univocal information on the site of the monomer ring opening. The numerical solution of equations given in Table 2 with respect to  $P_a$ ,  $P_b$ , and  $P_c$ , using experimental triad distributions showed that neither in the polymerization system in question is the condition  $P_{\text{main}} \approx 1$  fulfilled (Table 4). Therefore, this simple approach may be used when the regioselectivity is relatively high.

A more rigorous analysis was made on the basis of Markov statistics. According to the first-order Markovian chain, the way of the monomer opening depends only on the ultimate monomer unit in the polymer chain (Schemes 1 and 5). An additional simplification has been made that only the last siloxane group (X or D) affects the probability of monomer addition. Thus, the conditional probabilities of monomer addition to the  $\sim$ XDD and  $\sim$ DXD chain ends are the same. On the basis of these assumptions, sets of equations (Scheme 6) were derived for triad and pentad distributions. To analyze the pentad distribution, two subsequent additions of monomer were considered (Scheme 5).

The equations were solved with respect to the conditional probabilities of ring opening by a numerical minimization of the sum of squared deviations of calculated triad or pentad fractions from the corresponding experimental values (see Experimental Section). The fractions of monomer openings,  $P_a$ ,  $P_b$ , and  $P_c$ , were calculated from the conditional probabilities. An analysis of the triads did not provide any sufficient

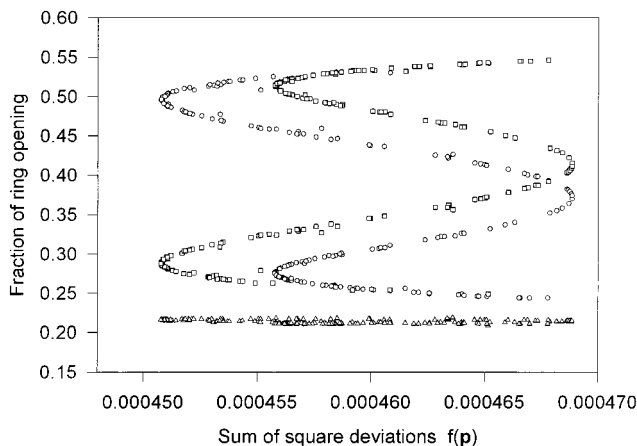


**Figure 4.** Dependence of fractions of ring opening,  $P_a$ ,  $P_b$ , and  $P_c$ , on the sum of squares deviation  $f(\mathbf{p})$ , obtained by numerical simulation (see Experimental Section) for the polymerization of **1** initiated by  $-\text{SiONMe}_4$  in toluene: ○,  $P_a(\text{XDD})$ ; □,  $P_b(\text{DDX})$ ; △,  $P_c(\text{DXD})$ . The most likely fractions of ring openings for a given experiment are those for which the sum  $f(\mathbf{p})$  reaches minimum. Two approximately equivalent symmetrical solutions are present in which the values of  $P_a$  and  $P_b$  are interchanged, that is, 0.50, 0.28, and 0.22 and 0.27, 0.51, and 0.22 for  $P_a$ ,  $P_b$ , and  $P_c$ , respectively.

information to obtain a unique solution of the equation system. Therefore, a more precise analysis was performed at the pentad level. Because the solution depends on the accuracy of the experimentally measured polymer sequencing, the shape of the deviation function was examined by a partial minimization procedure. In this way, a global minimum for each experiment was found (see Experimental Section). An example of this procedure is presented in Figure 4.

Because of the symmetry of the function, if  $P(\text{DDX}) \neq P(\text{XDD})$ , there is a pair of symmetrical solutions in which the values of both fractions of ring opening are interchanged. In some cases, more than two symmetrical solutions exist. For example, when  $P_a$  or  $P_b$  is equal to 0, four sets of the  $P_a$ ,  $P_b$ , and  $P_c$  lead to the same sequence distribution. Thus, the Markov statistics, as the Bernoullian ones, do not permit unequivocal determination of the fractions of openings at a, b, and c. A method, complementary to the statistical analysis, was used to select the solution, according to which the chain propagation occurred. It was based on the determination of the sequences at the termini of the polymer chain.

**Analysis of the Sequence Unit Order at the Termini of the Polymer Chain.** For anionic polymerization of **1**, initiated with lithium or potassium silanolate, experiments of labeled initiation and termination were performed. In the initiation experiment, the polymerization was initiated with trimethylsilanolate which introduced the trimethylsiloxane group at the beginning of the chain (Scheme 2).

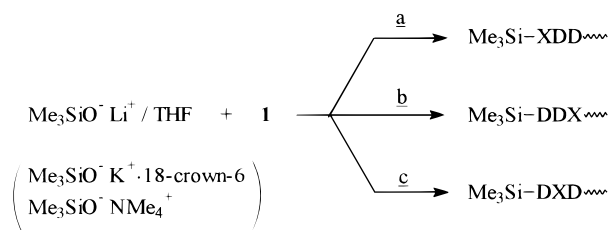


**Table 3.**  $^{29}\text{Si}\{^1\text{H}\}$  NMR Spectra of Model Compounds; Assignment of the  $\text{Me}_3\text{SiO}$  Signal for Various Neighborhoods and Tests of Quantitative Integration

no.	compound formula	chemical shifts (ppm)			percentage of total integration of signals found and theoretical		
		$\delta$ (1)	$\delta$ (2)	$\delta$ (3)	1	2	3
1	$\text{Me}_3\text{Si}^1\text{OPh}_2\text{Si}^2\text{OSi}^4\text{Me}_3$	10.17	-46.73		33.46 (33.33)	66.69 (66.67)	
2	$(\text{Me}_3\text{Si}^1\text{OMe}_2\text{Si}^2\text{O})_2\text{Si}^3\text{Ph}_2$	7.54	-20.39	-48.58	39.01 (40.00)	40.71 (40.00)	20.27 (20.00)
3	$[\text{Me}_3\text{Si}^1\text{O}(\text{Me}_2\text{SiO})_2]_2\text{Si}^2\text{Ph}_2$	7.31	-48.44				
4	$(\text{Me}_3\text{Si}^1\text{OMe}_2\text{Si}^2\text{O})_2\text{Si}^3\text{Me}_2$	7.14	-21.59	-22.35	39.90 (40.00)	39.83 (40.00)	20.27 (20.00)
5	$[(\text{Me}_2\text{Si}^1\text{O})_2\text{Ph}_2\text{Si}^2\text{O}]$	-6.63	-36.72		66.54 (66.67)	33.46 (33.33)	
6	$[\text{Me}_2\text{Si}^1\text{OMe}_2\text{Si}^2\text{OMe}_2\text{Si}^4\text{OPh}_2\text{Si}^3\text{O}]$	-17.45	-18.43	-46.34	49.90 (50.00)	25.00 (25.00)	25.10 (25.00)
7	$\sim[(\text{Me}_2\text{Si}^1\text{O})_2\text{Ph}_2\text{Si}^2\text{O}]_n\sim$	-19.3 -21.9	-47.4 -48.4		67.18 (66.67)	32.82 (33.33)	

**Table 4.** Comparison of Results of Statistical Analysis and Analysis of Chain Termini of Sequences of Siloxane Units in Poly( $\text{Me}_2\text{SiO-co-Ph}_2\text{SiO}$ ) Obtained by Anionic ROP of Monomer 1 (Fractions of Openings at a, b, and c (Schemes 1 and 2); Underlined Are Selected Solutions)

no.	polymerization system propagation center/solvent/ temp.	analysis of triads Bernoulli statistics			analysis of pentads Markov first-order statistics			analysis of chain termini <sup>a</sup>		
		a	b	c	a	b	c	a	b	c
1	$\sim\text{R}_2\text{SiOLi/THF/50 } ^\circ\text{C}$	0.73 0 <u>0-0.27</u>	0 0.73 <u>0-0.27</u>	0.26 0.26 0.73	0.17 0.35 <u>0.17</u>	0.35 0.17 <u>0.48</u>	0.48 0.48 <u>0.48</u>	0.33	0.18	0.49
2	$\sim\text{R}_2\text{SiOK} + 18\text{-crown-6 } 1:1/\text{toluene/50 } ^\circ\text{C}$	0.79 0.09	0.09 0.79	0.11 0.11	0.72 0.13	0.13 0.72	0.15 0.15	0.10	0.73	0.17
3	$\sim\text{R}_2\text{SiONMe}_4/\text{toluene/30 } ^\circ\text{C}$	0.73 0.10	0.10 0.73	0.17 0.17	0.50 0.28	0.28 0.50	0.22 0.22			

<sup>a</sup> From initiation experiment.**Scheme 2**

The polymerization was quenched by washing out the base with a large amount of water which transformed the active propagation center into the silanol group. The  $^{29}\text{Si}$  chemical shift of the  $\text{Me}_3\text{Si}$  extremity of the polymer depends on the order of siloxane units in the neighboring triad, formed from the monomer added to the initiator. Thus, the fractions of the opening of the monomer ring at sites a, b, and c by the initiator may be directly determined. The assignment of signals of the  $\text{Me}_3\text{Si}$  group, bonded to the three respective triads, was made using model oligomers, see Table 3.

Because the structure of the initiator is similar to that of the active propagation center, the results of the initiation experiment may be used to select the set of  $P_a$ ,  $P_b$ , and  $P_c$  values, according to which the chain propagation occurs, from the two solutions provided by the Markov analysis. The results of the initiation experiments are compared with those obtained from the statistical methods in Table 4. Indeed, for each of the systems studied there is one numerical solution of equations, which fits the initiation experiment.

The termination experiment with  $\text{Me}_3\text{SiCl}$ , which introduced the  $\text{Me}_3\text{Si}$  group at the end of the chain, was performed for the polymerization of **1** initiated with dilithium disiloxanolate. Because termination is much

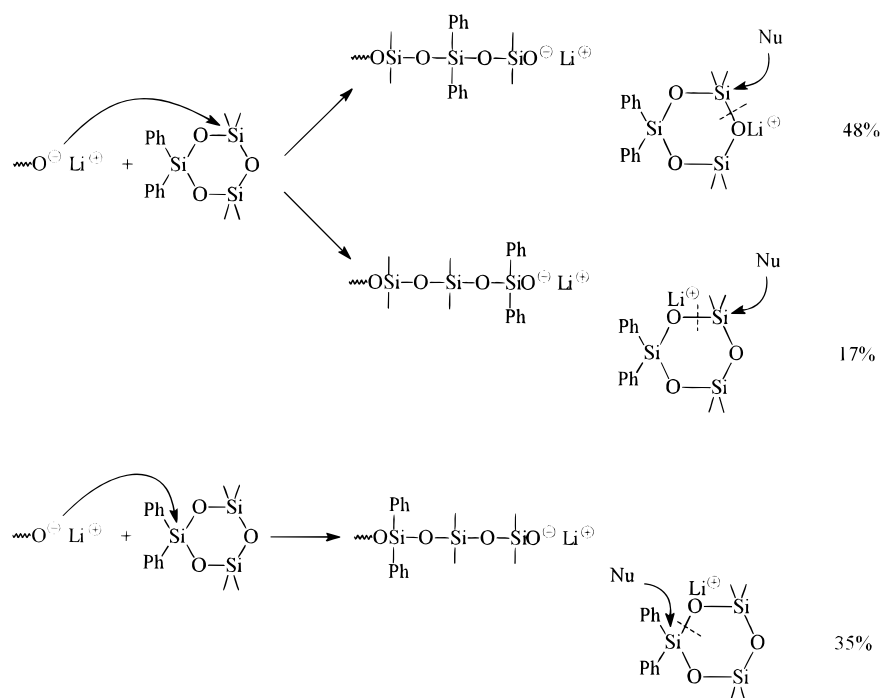
**Table 5.** Comparison of Instantaneous Relative Orders of Units at Active Propagation Center Found from Termination Experiment with Relative Orders of Units inside the Chain from Markov Analysis

	fraction of order inside the chain	fraction of order at the active propagation center	approximate relative rates $k_{\text{SiMe}_2\text{O}^-\text{Li}^+}/k_{\text{SiPh}_2\text{O}^-\text{Li}^+}$
$\begin{array}{c} \text{Ph} \\   \\ \text{Si} \text{---} \text{O} \text{---} \text{Si} \text{---} \text{O} \text{---} \text{Si} \text{---} \text{O} \text{---} \\   \quad   \quad   \\ \text{Ph} \quad \text{Ph} \quad \text{Ph} \end{array}$	0.35	0.22	
$\begin{array}{c} \text{Ph} \\   \\ \text{Si} \text{---} \text{O} \text{---} \text{Si} \text{---} \text{O} \text{---} \text{Si} \text{---} \text{O} \text{---} \\   \quad   \quad   \\ \text{Ph} \quad \text{Ph} \quad \text{Ph} \end{array}$	0.17	0.46	$\sim 4$
$\begin{array}{c} \text{Ph} \\   \\ \text{Si} \text{---} \text{O} \text{---} \text{Si} \text{---} \text{O} \text{---} \text{Si} \text{---} \text{O} \text{---} \\   \quad   \quad   \\ \text{Ph} \quad \text{Ph} \quad \text{Ph} \end{array}$	0.48	0.32	

faster than propagation, see for example ref 25, the experiment permits estimation of the relative stationary concentrations of the active propagation centers. The results do not agree with those obtained by the statistical method, representing the order of siloxane units in monomer units inside the chain (Table 5), because the stationary concentrations of active propagation centers also depend on their reactivities. Thus, the fraction of monomer units  $\rightarrow\text{DDX}\rightarrow$  obtained from the quenching experiment, 0.46, is much higher than that from the initiation experiment, 0.18, and that from the statistical analysis, 0.17, because of a lower reactivity of the  $\sim\text{Ph}_2\text{SiO}^-\text{Li}^+$  propagation center. The latter reacts  $\approx 4$  times slower than the former, as may be estimated by comparison of the results of both the initiation and quenching experiments.

**The Mechanism of Propagation.** As was discussed in Mazurek et al.'s paper,<sup>9</sup> phenyl substituents in

Scheme 3



monomer **1** are expected to affect the site of the ring opening by (1) making the nucleophilic attack at silicon easier, (2) stabilizing the new silanolate center formed in the reaction, and (3) modifying the interaction of the monomer with the counterion of the propagation center. The site of the opening depends on which of these factors is the most important.

On the basis of inductive effects, the nucleophilic attack of the silanolate anion is expected to be directed to the most electrophilic silicon center which is the silicon bonded to phenyl groups. However, only 35% of the propagation on lithium silanolate proceeds by this route. (Scheme 3) The attack on the dimethylsilyl group is privileged. The attack results mostly in the cleavage of the siloxane bond opposite to the diphenylsilyl group (route c), thus forming a symmetrical DXD arrangement of siloxane units in the added open chain monomer. This is evidence for the role of the lithium counterion in the propagation. The cation assists ring opening by interaction with siloxane oxygen. The assistance was postulated earlier<sup>9</sup> and was confirmed by recent *ab initio* calculations.<sup>26,27</sup> Considering the inductive effect of phenyl groups, the most effective interaction of the lithium cation should be the one with oxygen bridging two dimethylsilyl groups, which would explain the observed tendency to symmetrical ring opening. However, the attack on the  $\text{Me}_2\text{Si}$  group proceeds partially with the cleavage of the siloxane bond linking the diphenylsilyl group with the  $\text{Me}_2\text{Si}$  one, which leads to a  $\rightarrow\text{DDX}\rightarrow$  arrangement. The driving force for this ring opening is a higher stability of the siloxydiphenylsilanolate.

The potassium cation in a complex with a crown ether, as well as the tetraammonium cation, may interact with cyclosiloxane in a way more restricted than the lithium cation in THF. Thus, the symmetrical opening, driven by the monomer–cation interaction, is less important in these cases. However, the nucleophilic attack of silanolate is again predominantly directed toward the dimethylsilyl group, leading to the DDX opening. This

result shows that the stabilization of the silanolate product may be more important than the electrophilicity of the silicon in the siloxane substrate as a factor governing the direction of the nucleophilic attack of silanolate on a cyclosiloxane which suggests a late transition state. A similar conclusion may be drawn from the observation of Kawakami et al. that in the anionic polymerization of 2,2-dimethyl-5-naphthyl-5-phenyl-1-oxa-2,5-disilacyclopentane the ring opening predominantly occurs with the formation of a more stable naphthylphenylalkylsilanolate.<sup>28</sup>

To better understand the role of the monomer–cation interaction, *ab initio* calculations were performed for the two structures of the monomer–metal cation complex, that is, the structure involving potassium or lithium coordinated to oxygen, bridging two dimethylsilyl groups, and the one with potassium or lithium interacting with oxygen at the diphenylsilyl group. The structures, optimized at HF/3-21G\* to the lowest energies, are presented in Scheme 4.

Unexpectedly, the isolated structures with a cation at oxygen bonded to the diphenylsilyl group proved to be more stable, because of a direct interaction with the phenyl group. The interaction of the lithium cation is of  $\sigma$ -type, involving the ipso carbon of the phenyl group. A similar interaction of the lithium cation with the phenyl ipso carbon was observed by Eaborn et al. in a tris(phenyldimethylsilyl)methyl lithium complex.<sup>29</sup> The excess energy of the unsymmetrical structure, due to this interaction, is perhaps overestimated at this level of theory. The interaction of phenyl with the potassium cation is of  $\pi$ -type ( $\eta^6\pi$ ), involving the entire phenyl ring (structures C and D in Scheme 4). In contrast to lithium, the potassium cation, coordinated to oxygen between the dimethylsilyl groups, is also able to interact with phenyl. Although this interaction is weaker, it distorts the nearly planar geometry of the monomer ring (Scheme 4, structure C). The significance of these calculations should not be overestimated as they were made for isolated molecules in a vacuum. Ion interaction with a

Scheme 4

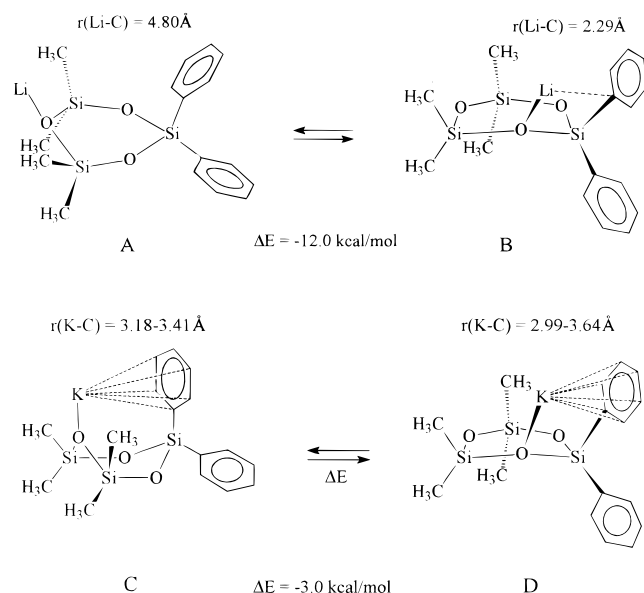


**Table 6. Comparison of the Cleavage of the Model Monomer Ring by  $\sim\text{SiMe}_2\text{O}^- \text{Mt}^+$  and  $\sim\text{SiPh}_2\text{O}^- \text{Mt}^+$**

Mt <sup>+</sup>	silanolate anion	percentage opening		
		a	b	c
Li <sup>+</sup> (THF)	$\sim\text{SiMe}_2\text{O}^-$	41	8	51
	$\sim\text{SiPh}_2\text{O}^-$	4	61	35
K <sup>+</sup> (crown)	$\sim\text{SiMe}_2\text{O}^-$	16	74	10
	$\sim\text{SiPh}_2\text{O}^-$	12	73	15
NMe <sub>4</sub> <sup>+</sup>	$\sim\text{SiMe}_2\text{O}^-$	35	43	22
	$\sim\text{SiPh}_2\text{O}^-$	23	56	21

solvent or promoter may considerably change the character and the role of the cation–monomer interaction in the polymerization process. Anyway, the results of the calculations point to a possible role of the interaction of counterions with substituents at silicon in the ring opening. In particular, they may stabilize the transition state of the ring opening at site b (Schemes 1 and 2), leading to the formation of the more stable silanolate structure.

The values of conditional probabilities are worth a closer analysis as they give information about the preferences in an attack of dimethylsilanolate and diphenylsilanolate propagation centers on various sites of the monomer ring. Conditional probabilities  $p_{a/(a+c)}$ ,  $p_{b/(a+c)}$ ,  $p_{c/(a+c)}$ ,  $p_{a/b}$ ,  $p_{b/b}$ , and  $p_{c/b}$  in terms of the respective percentage of the ring opening at a, b, and c are presented in Table 6. The data indicate that the lithium siloxydiphenylsilanolate chooses main route b, leading to the reformation of the same silanolate while the lithium siloxydimethylsiloxanolate prefers to open the monomer ring at site a. This crossover in the reactivity order may be explained by the different characters of the ion pairs of both propagation centers. The siloxydimethylsilanolate–lithium ion pair is intimate where the ions are bonded by strong electrostatic attractive forces. The assistance of the counterion in the ring opening is more important; thus, the transition state occurs earlier than that in the case of the siloxane cleavage by siloxanediphenylsilanolate. In the latter, the cation is bonded more loosely and, consequently, the transition state occurs later, according to route b, that is, in the place where the most stable center is formed. In the crown ether complex of both potassium silanolates the counterion is only loosely bonded and both

siloxydimethylsilanolate and siloxydiphenylsilanolate prefer route b.

An alternative explanation invoking the steric effect must also be taken into account as the lithium cation coordinated to oxygen and the phenyl group of the monomer may make the nucleophilic attack of the siloxydiphenylsilanolate at diphenylsiloxane unit more difficult.

This crossover in the reactivity order of lithium silanolates does not contradict the conclusion drawn from the initiation experiment. The structure of the initiator used in this experiment,  $\text{Me}_3\text{SiO}^- \text{Li}^+$ , is close to that of  $\sim\text{SiMe}_2\text{O}^- \text{Li}^+$  propagation centers which accounts for 83% of the building of the monomer.

## Conclusions

The sequential analysis of siloxane units in a copolymer, formed in the ring-opening polymerization of a cyclotrisiloxane with mixed units, is a good diagnostic tool for the chemoselectivity of polymerization. The anionic polymerization of 2,2,4,4-tetramethyl-6,6-diphenylcyclotrisiloxane in the three systems studied here, that is, with propagation on lithium silanolate in THF, on potassium silanolate-18-crown-6 complex in toluene, and on tetramethylammoniumsilanolate in toluene, proceeds chemoselectively and is not affected by the processes of polymer chain cleavage, up to a high conversion of the monomer.

A precise analysis of the composition of sequences at the level of pentads for the copolymer obtained by the chemoselective process allows estimation of the regioselectivity of the polymerization. Calculations were based on the Markov chain statistics, using sequences at the pentad level. An additional experiment of initiation of the polymerization by trimethylsilanolate ion, having the structure corresponding to that of the propagation ion, made it possible to select the solution obtained from the Markov statistics, according to which the propagation occurs.

The quantitative analysis of the regioselectivity gives precise information about the site of the opening of the monomer ring in propagation, thus providing important information on the mechanism of polymerization. In particular, the results point to a considerable role of the two kinds of interactions of the counterion with a monomer, giving assistance to the ring opening, that is, the association with siloxane oxygen and the coordination to the phenyl group. The stabilization of the silanolate product by phenyl groups may also be important in choosing the method of monomer addition to the growing polymer chain.

## Experimental Section

**Chemicals.** (1) **Solvents Used for Syntheses.** THF, toluene, and *n*-heptane were purified according to standard methods described in ref 30. They were stored in an ampule with a Rotaflo stopcock under dry argon.

(2) **Monomer.** 2,2,4,4-Tetramethyl-6,6-diphenylcyclotrisiloxane, **1**, prepared according to the procedure described in ref 31, was purified by recrystallization from *n*-heptane and distillation on a high vacuum line ( $10^{-3}$  mmHg, bp 80–85 °C).

(3) **Initiators.** All operations with initiators were performed with care to prevent any contact with the atmosphere, using a high vacuum or inert gas techniques. Potassium trimethylsilanolate was prepared by reaction of trimethylsilanol with potassium in toluene. The complex with 18-crown-6 was

prepared by mixing the crown ether in equimolar proportion with  $\text{Me}_3\text{SiOK}$  in toluene.

**(4) Lithium Trimethylsilanolate.** Lithium trimethylsilanolate was synthesized by reacting hexamethylcyclotrisiloxane with methylolithium solution in diethyl ether (Aldrich) according to the method described in ref 30.

**(5) 1,3-Dilithium Tetramethyldisiloxane-1,3-diolate.** 1,3-Dilithium tetramethyldisiloxane-1,3-diolate was prepared in an analogous way to that used in the preparation of  $\text{Me}_2\text{Si}(\text{OLi})_2$ .<sup>32</sup>

**(6) Bis-tetramethylammoniumoligodimethylsiloxane- $\alpha,\omega$ -diolate.**  $\text{Me}_4\text{N}(\text{OSiMe}_2)_n\text{ONMe}_4$ ,  $n = 4$ , was synthesized according to the description in ref 33.

**(7) Model Oligosiloxanes for  $^{29}\text{Si}$  NMR Studies.** 1,1,1,5,5,5-Hexamethyl-3,3-diphenyltrisiloxane, 1,1,1,3,3,7,7,9,9,9-decamethyl-5,5-diphenylpentasiloxane, 1,1,1,3,3,5,5,9,9,11,11,13,13,13-tetradecamethyl-7,7-diphenylheptasiloxane, and 2,2,4,4,6,6-hexamethyl-8,8-diphenylcyclotetrasiloxane were obtained by heterofunctional condensation from  $\text{Ph}_2\text{SiCl}_2$  and the corresponding oligopermethyldisiloxanol using  $\text{Et}_3\text{N}$  as the hydrogen acceptor and 4-dimethylaminopyridine as the catalyst.<sup>34</sup>

**Polymerization.** Polymerization of monomer **1** was carried out in a thermostated 50-mL glass Schlenk type reactor under prepurified argon. The solution of  $1.2 \text{ mol dm}^{-3}$  of monomer **1** in toluene or in THF was placed in the reactor thoroughly purged with argon. The solution contained a known amount of *n*-dodecane which served as a standard for gas chromatographic analysis. The initiator ( $10^{-2} \text{ mol dm}^{-3}$ ) was introduced with a Hamilton precision syringe to the solution under a flow of argon at  $30^\circ\text{C}$ . The polymerization was followed by sampling and gas chromatographic analysis. The reaction was quenched at the monomer conversion of 60–90% by introduction of a small excess of  $\text{Me}_3\text{SiCl}$ . In the case of fast reactions, the time of quenching was determined in separate polymerization experiments. The polymer solution was washed several times with water and dried over  $\text{CaCl}_2$ . Then the solvent was evaporated and the polymer was dissolved in  $\text{CH}_2\text{Cl}_2$ . Cyclics were separated from the linear polymer by repetitive precipitation with methanol. The polymer was dried by heating on a vacuum line and was characterized by SEC and NMR spectroscopy. The molecular weight of the polymers,  $\bar{M}_n$ , was about  $2 \times 10^4$ .

In the initiation experiment the polymerization was initiated by  $5 \times 10^{-2} \text{ mol dm}^{-3}$  of lithium trimethylsilanolate and quenched by adding a large excess of distilled water to the polymerization system vigorously stirred by means of a magnetic stirrer.

In the quenching experiment the polymerization was initiated with dilithium tetramethyldisiloxanolate and quenched with an excess of trimethylchlorosilane–triethylamine mixture.

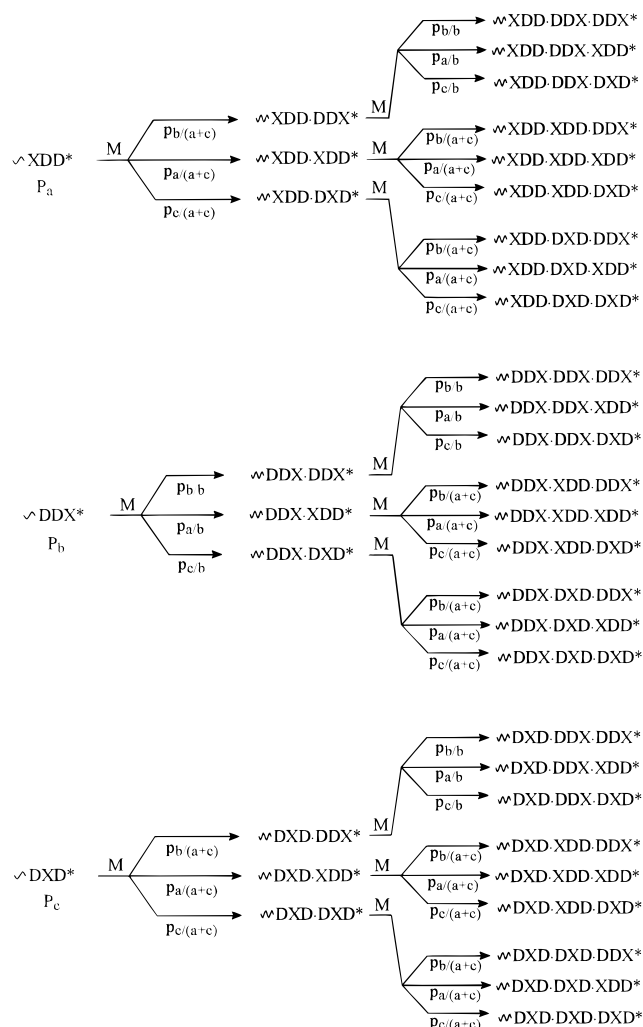
**Analysis.**  $^{29}\text{Si}$  NMR spectra were taken with a Bruker MSL 300 spectrometer using  $\text{CDCl}_3$  as the solvent. A good resolution of pentads and quantitative integration was achieved by the addition of  $\text{Cr}(\text{acac})_3$  and use of a gated decoupling technique. The spectral parameters were selected using model compounds (Table 3). A pulse delay of 15 s and pulse length of  $15 \mu\text{s}$  were typically applied.

Gas chromatography analysis and SEC analysis were made using the procedure described earlier.<sup>35</sup>

**Computational Methods. (1) Numerical Analysis.** Equations describing triad and pentad distribution were numerically solved with respect to the conditional probabilities of the three ways of monomer addition. The equation sets for triad and pentad distribution, derived assuming first-order Markov statistics, are presented in Schemes 5 and 6.

Algebraic transformations with the Mathematica program (Wolfram Research, Inc.) allowed reduction of the number of independent variables (conditional probabilities of ring opening) to four (Scheme 6). The optimization algorithm utilizes a nonlinear least-squares approach with the nongradient

Scheme 5



Rosenbrock method<sup>36</sup> to minimize the squared deviation function,  $f$ , defined as

$$f(\mathbf{p}) = \sum_{\text{all pentads}} ([Y_1 Y_2 Y_3 Y_4 Y_5]_{\text{calc}} - [Y_1 Y_2 Y_3 Y_4 Y_5]_{\text{exp}})^2$$

where  $[Y_1 Y_2 Y_3 Y_4 Y_5]_{\text{calc}}$  are fractions of pentads calculated, according to the above equations, and  $[Y_1 Y_2 Y_3 Y_4 Y_5]_{\text{exp}}$  are fractions of pentads in a polymer, estimated by  $^{29}\text{Si}$  NMR;  $\mathbf{p}$  is a set of conditional probabilities for a given model.

The absolute deviations, instead of relative values, are taken to the function  $f$ , which implies that highly populated pentads are treated with a greater weight by the optimization procedure. This is reasonable since the measured concentrations of low-populated pentads are charged with larger error.

The user provides a starting estimate solution which is then automatically optimized, giving the values of the conditional probabilities as well as the total fractions of the three monomer openings,  $P_a$ ,  $P_b$ , and  $P_c$ . Numerical analysis shows a fairly good agreement with the experimental pentad distribution for most of the experiments. However, the minimized function depends on the accuracy of the experimentally measured polymer sequencing.

To ensure that all the possible solutions were correctly found, the behavior of the function was examined over the full space of conditional probabilities, using two independent procedures. In the first one, the squared deviation function,  $f(\mathbf{p})$ , was minimized for the starting parameters, which varied regularly from 0 to 1, with a constant step of 0.1. Depending on the starting parameters, the program stopped the search for the minimum, according to the defined convergence



## Scheme 6

## Analysis of triads

$$\begin{aligned}
3([XDD]+[DDX]) &= P_b(1+p_{bb})+P_a(1+p_{a(a+c)}+p_{c(a+c)})+P_c(p_{b(a+c)}+2p_{c(a+c)}) \\
3([DDD]) &= P_a(2p_{b(a+c)}+p_{c(a+c)})+P_c p_{b(a+c)} \\
3([DXD]) &= P_b(p_{bb}+p_{cb})+P_a p_{a(a+c)}+P_c(1+p_{a(a+c)}) \\
3([XDX]) &= P_b p_{cb}+P_a p_{a(a+c)} \\
3([DXX]+[XXD]) &= 2P_b p_{ab}
\end{aligned}$$

## Analysis of pentads

$$\begin{aligned}
3([XDDDD]+[DDDDX]) &= 2P_a p_{b(a+c)} \\
3([DXDDD]+[DDDXD]) &= P_a(p_{a(a+c)}(p_{b(a+c)}+p_{c(a+c)})+p_{b(a+c)}(p_{bb}+p_{cb})+p_{c(a+c)})+ \\
&\quad P_c(p_{a(a+c)}(p_{c(a+c)}+p_{b(a+c)})+p_{b(a+c)}(p_{bb}+p_{cb}+1)) \\
3([DXXDD]+[DDXXD]) &= 2P_b p_{ab} \\
3([XDDXD]+[DXDDX]) &= P_a p_{a(a+c)}(1+p_{a(a+c)})+P_b p_{bb}(1+p_{bb}+p_{cb})+P_c(p_{a(a+c)}^2+2p_{c(a+c)}) \\
3([XDXDD]+[DDXDX]) &= P_a p_{a(a+c)} p_{c(a+c)}+P_b p_{cb}(p_{b(a+c)}+p_{c(a+c)}+1)+P_c p_{a(a+c)}(p_{c(a+c)}+1) \\
3([XXDDD]+[DDDDX]) &= p_{ab}(p_{b(a+c)}+P_a p_{c(a+c)}) \\
3([XDDXX]+[XXDDX]) &= P_b p_{ab}(p_{bb}+p_{a(a+c)}) \\
3([DDXDD]) &= P_a(p_{a(a+c)}+p_{c(a+c)}(p_{b(a+c)}+p_{c(a+c)}))+P_b p_{bb}+P_c p_{c(a+c)}(p_{b(a+c)}+p_{c(a+c)}) \\
3([DXDXD]) &= P_b p_{cb}+P_a p_{a(a+c)} \\
3([XDDDX]) &= P_a p_{c(a+c)}+P_c p_{b(a+c)} \\
3([XDXDX]) &= P_b p_{a(a+c)} p_{cb}
\end{aligned}$$

where the following conditions are fulfilled:

$$\begin{aligned}
p_{b(a+c)}+p_{a(a+c)}+p_{c(a+c)} &= 1 \\
p_{ab}+p_{bb}+p_{cb} &= 1 \\
P_a &= p_a p_{ab}+(P_a+P_c)p_{a(a+c)} \\
P_b &= p_b p_{bb}+(P_a+P_c)p_{b(a+c)} \\
P_c &= p_c p_{cb}+(P_a+P_c)p_{c(a+c)} \\
P_a+P_b+P_c &= 1
\end{aligned}$$

criterion, at different points close to the local minima. The resulting values of  $f(\mathbf{p})$  were then stored together with the corresponding optimal values of conditional probabilities and fractions of ring opening. A global minimum of the function  $f(\mathbf{p})$  could be found in this way. An example of the dependence of  $P_a$ ,  $P_b$ , and  $P_c$  on  $f(\mathbf{p})$  for the experiment, using the  $-\text{SiONMe}_4$  propagation center in toluene, is presented in Figure 4.

The second verification procedure involved the generation of a polymer chain by the Monte Carlo method, using numerically calculated conditional probabilities.

**(2) Monte Carlo Simulation.** In that procedure, the polymer chain growth was simulated, assuming the conditional probabilities of monomer ring opening.

The resulting triad and pentad distributions agreed very well with the values optimized by the numerical method. The calculated pentad fractions are compared with those found experimentally in Table 1.

Both the numerical analyses and Monte Carlo simulations were run on a PC computer, using programs written in Borland Pascal (Borland, Inc.).

**(3) Quantum Mechanical Calculations.** Ab initio calculations were carried out using standard techniques,<sup>37</sup> as implemented in the *Gaussian 94* series of the programs.<sup>38</sup> Equilibrium geometries and energies of cyclic siloxonium ions, resulting from an addition of the metal cation to the monomer, were calculated at the Hartree–Fock level, using the polarized 3-21G\* basis set.

**Acknowledgment.** Authors are indebted to Mrs. Teresa Barczyńska for her assistance in the preparation of the manuscript of this paper. This research was supported by the State Committee for Scientific Studies (KBN) Grant 3T09A 03015.

## Appendix

A general scheme of reactions considered in the first-order Markov analysis of triads and pentads is shown in Scheme 5. The conditional probabilities of monomer addition are marked under arrows. Assumption is made that the probabilities depend on the structure of the last siloxane unit only.

The analysis of the reactions in Scheme 1 leads to the equations for triad and pentad distributions presented in Scheme 6.

## References and Notes

- (1) Partly presented at the International Symposium on Ionic Polymerization, Paris, France 1997. Kaźmierski, K.; Cypryk, M.; Chojnowski, J. *Macromol. Symp.* **1998**, *132*, 405.
- (2) Kendrick, T. C.; Parbhoo, B.; White, J. W. In *The Silicon-Heteroatom Bond*; Armitage, D. A., Corriu, R. J. P., Kendrick, T. C., Parbhoo, B., Tilley, T. D., White, J. C., Eds.; J. Wiley and Sons: Chichester 1991; p 67.
- (3) Kennan, J. J. In *Siloxane Polymers*; Clarson, S. J., Semlyen, J. A., Eds; Ellis Horwood PTR Prentice Hall: Englewood Cliffs, NJ, 1993; Chapter 2, p 72.
- (4) Kendrick, T. C.; Parbhoo, B.; White, J. W. In *The Chemistry of Organic Silicon Compounds*; Patai, S., Rappoport, Z., Eds; J. Wiley and Sons: Chichester, 1989; p 1289.
- (5) Kobayashi, H.; Nishiumi, W. *Makromol. Chem.* **1993**, *194*, 1403.
- (6) Ziemelis, M. J.; Saam, J. C. *Macromolecules* **1989**, *22*, 2111.
- (7) Spinu, M.; McGrath, J. E. *J. Polym. Sci., Part A: Polym. Chem.* **1991**, *29*, 657.
- (8) Wright, P. V.; Beevers, M. S. In *Cyclic Polymers*; Semlyen, J. A., Ed.; Elsevier: London, 1986; p 85.
- (9) Mazurek, M.; Ziętera, J.; Sadowska, W.; Chojnowski, J. *Makromol. Chem.* **1980**, *181*, 777.
- (10) Andrianov, K. A.; Zavin, B. G.; Sablina, G. F. *Vysokomol. Soedin.* **1972**, *A14*, 1156.
- (11) Laita, Z.; Jelinek, M. *Vysokomol. Soedin.* **1963**, *5*, 1268.
- (12) Cazacu, M.; Marcu, M.; Petrovan, S.; Lazarescu, S. *J. Macromol. Sci. Chem.* **1996**, *A33*, 65.

- (13) Herczyńska, L.; Chojnowski, J.; Lacombe, L.; Lestel, L.; Polowiński, S.; Boileau, S. *J. Polym. Sci. Part A: Polym. Chem.* **1998**, *36*, 137.
- (14) Andrianov, K. A.; Yakushkina, S. E.; Koretko, I. I.; Lavrukhin, B. D.; Petrova, I. I. *Vysokomol. Soedin., Ser. A* **1971**, *13*, 2754.
- (15) Różga-Wijas, K.; Chojnowski, J.; Zundel, T.; Boileau, S. *Macromolecules* **1996**, *29*, 2711.
- (16) Meier, D. J.; Lee, M. K. *Polymer* **1993**, *34*, 4882.
- (17) Baratova, T. N.; Mileshekevich, V. P.; Gurari, V. I. *Vysokomol. Soedin.* **1983**, *A25*, 2497.
- (18) Fortuniak, W.; Chojnowski, J. *Polym. Bull.*, **1997**, *38*, 371.
- (19) Hempenius, M. A.; Lammerting, M. G. H.; Vansco, G. L. *Macromolecules* **1997**, *30*, 266.
- (20) Różga-Wijas, K.; Chojnowski, J.; Boileau, S. *J. Polym. Sci. Part A: Polym. Chem.* **1997**, *35*, 879.
- (21) Chojnowski, J.; Różga, K. *J. Inorg. Organomet. Chem.* **1992**, *2*, 297.
- (22) Jancke, H.; Englehardt, G.; Kriegerman, H.; Keller, F. *Plaste Kautschuk* **1979**, *26*, 612.
- (23) Chojnowski, J. In *Siloxane Polymers*; Clarson, S. J., Semlyen, J. A., Eds.; Ellis Horwood PTR Prentice Hall: Englewood Cliffs, NJ, 1993; Chapter 1, p 1.
- (24) Mazurek, M.; Chojnowski, J. *Makromol. Chem.*, **1977**, *178*, 1005.
- (25) Wilczek, L.; Kennedy, J. P. *Polym. J.* **1987**, *19*, 531.
- (26) Kress, J. D.; Leung, P. C.; Tawa, G. J.; Hay, P. J. *J. Am. Chem. Soc.* **1997**, *119*, 1954.
- (27) Kress, J. D.; Leung, P. C.; Tawa, G. J.; Hay, P. J. *Polym. Prepr. (Am. Chem. Soc., Div. Polym. Chem.)* **1998**, *39*, 446.
- (28) Li, Y.; Kawakami, Y. *Macromolecules* **1999**, *32*, 548.
- (29) Eaborn, C.; Hitchcock, P. B.; Smith, J. D.; Sullivan, A. C. *J. Chem. Soc., Chem. Commun.* **1983**, 1390.
- (30) Perrin, D. D.; Armarego, W. L. F.; Perrin, D. R. *Purification of Laboratory Chemicals*; Pergamon Press: New York, 1980.
- (31) Frye, C. L.; Salinger, R. M.; Fearon, F. W. G.; Klosowski, J. M.; De Young, T. *J. Org. Chem.* **1970**, *35*, 1308.
- (32) Gnanou, Y.; Rempp, P. *Makromol. Chem.* **1988**, *189*, 1997.
- (33) Gilbert, A. R.; Kantor, S. W. *J. Polym. Sci.* **1959**, *40*, 3558.
- (34) Rubinsztajn, S.; Cypriak, M.; Chojnowski, J. *J. Organomet. Chem.* **1989**, *367*, 27.
- (35) Kurjata, J.; Scibiorek, M.; Fortuniak, W.; Chojnowski, J., *Organometallics* **1999**, *18*, 1259.
- (36) Rosenbrock, H. H. *Comput. J.* **1960**, *3*, 175.
- (37) Hehre, W. J.; Radom, L.; Schleyer, P. v. R.; Pople, J. A. *Ab Initio Molecular Orbital Theory*; J. Wiley & Sons: New York, 1986.
- (38) Frisch, M. J.; Trucks, G. W.; Schlegel, H. B.; Gill, P. M. W.; Johnson, B. G.; Robb, M. A.; Cheeseman, J. R.; Keith, T.; Petersson, G. A.; Montgomery, J. A.; Raghavachari, K.; Al-Laham, M. A.; Zakrzewski, V. G.; Ortiz, J. V.; Foresman, J. B.; Cioslowski, J.; Stefanov, B. B.; Nanayakkara, A.; Challacombe, M.; Peng, C. Y.; Ayala, P. Y.; Chen, W.; Wong, M. W.; Andres, J. L.; Replogle, E. S.; Gomperts, R.; Martin, R. L.; Fox, D. J.; Binkley, J. S.; Defrees, D. J.; Baker, J.; Stewart, J. P.; Head-Gordon, M.; Gonzalez, C.; Pople, J. A. *Gaussian 94*, revision C.2; Gaussian, Inc.: Pittsburgh, PA, 1995.

MA9912610